BOWDEN TUBE NITI ACTUATORS
WITH LINEAR PARAMETER VARYING MODEL AND SLIDING MODE CONTROL

Austin Gurley*, Kyle Kubik, Tyler Ross Lambert, & David Beale
Department of Mechanical Engineering
Auburn University
Auburn, Alabama, USA

Royall Broughton
Department of Polymer and Fiber Engineering
Auburn University
Auburn, Alabama, USA

ABSTRACT

One of the primary difficulties to implementing NiTi shape memory alloys as robotic actuators is reliably amplifying their low linear strain to large effective displacements. Bowden tubes, called "push-pull cables" in other industries, allow a long length of Shape Memory Alloy (SMA) wire to fit in a small space; this provides a method for increasing effective SMA actuator strain without compromising space or complexity of the entire mechanism. The mechanical advantage of the Bowden tube provides faster actuation speeds, but comes at a cost of increased thermal capacitance resulting in higher power consumption. A feedback control system has been formed comprising the Bowden tube actuator, a rotary platform, and a microcontroller. The controller heats the SMA by passing current through the SMA wire using pulse-width-modulation. After describing the creation of the electro-mechanical system, its capabilities and limitations are discussed. Linear Parameter Varying (LPV) models of SMA are used to determine the range of characteristics the inherently nonlinear SMA system will exhibit. A sliding mode controller is designed based on these characteristics, and implemented in the prototype. Sliding-mode control is shown to be a powerful tool for SMA control even when system parameters are uncertain.

INTRODUCTION AND MOTIVATION

Many industrial, commercial, and robotic applications require small rotary actuators for operation. For small and lightweight applications, the RC "hobby" servo is often the actuator of choice, characterized by a small range of rotary motion with easy position control, in a small package, and at low cost. This work focuses on the implementation of NiTi wires as actuators for an equivalent rotary device. While the benefits of SMA are known in the research community, their benefits are not well known in industry. Designers are comfortable with the form and function of electromagnetic devices (like RC servos), and do not consider the unusual design requirements that would enable them to use smart materials. By creating an equivalent servo powered by SMA, we eliminate the design difficulty and make SMA devices accessible to designers and engineers worldwide. The members of the smart materials community know the general characteristics of NiTi wire so those will not be repeated here (c.f. [1, 2, 3, 4, 5]). The primary concern of this work is to create a strong rotary actuator with reliable position control. By using a Bowden tube mechanism, we are able to package a long length of NiTi wire in an unobtrusive manner. Secondarily, the actuator must be controlled. A microcontroller circuit is created to heat the SMA using Joule heating. A potentiometer provides position information for feedback control.

Typical NiTi variants have a reliable strain of 4% over a long lifetime. Even though this strain is very small, the stress created is very high and so the resulting specific energy (stress times stroke) is very high. There are three ways to amplify the strain of an SMA device: by creating leverage with mechanical strain, packaging more wire in the device so the total stroke of the wire increases, or a combination of the two. The choice is left to the designer, keeping in mind that stress and stroke can be interchanged without a loss of device energy, but that total energy (and energy consumption) increases when more total wire is included. There are many examples of strain

amplification using leverage [6], packaging more wire [7], and combinations of the two [8, 9, 10]. The particular method employed in this work uses a Bowden tube configuration. This technique is not popular in the smart materials community, though some examples are known [11]. It is commonly used in robotics where it allows heavy motors to drive motion at a distant location, where the mass would interfere with the device operation [12]. The details of our implementation are provided in the following section. The Bowden tube has interesting ramifications for heat transfer and power consumption. It provides a higher bandwidth than the SMA wire in ambient air, but requires more power because the tube itself is heated along with the SMA wire.

One-dimensional 'phenomenological' models for SMA wire devices have been explored and reviewed many times (c.f. [1, 4]). Control laws have also been thoroughly reviewed [13, 14]. Unfortunately, most of the controllers seen in the literature have no basis in a model of the material; they consider the principles characteristics of the behavior (hysteresis, etc.). A few draw meaningful conclusions from the model that improve control performance or accuracy [15, 16, 17, 18]. In this work, the focus is on reducing a simple model of SMA material into a form that provides insight into the controller design, allowing simpler controllers to be implemented that consider the model. In particular, a 'snapshot' of the actuator behavior is created using a 'linear parameter varying' modelling framework, with Martensite fraction determining the varying coefficients. Because the SMA devices are typically heated using electric current, sliding mode control has proven to be a reliable control method that requires little knowledge of the material to implement [19, 20, 18].

This paper begins by describing the Bowden tube mechanism design. Enough detail is provided that other researchers should be able to replicate the concept, as it has some significant benefits for adoption of SMA in many industries. These details include selection of the tube itself, the mechanical frame system, and the electrical control circuit. The performance of this mechanism is then characterized with particular focus on the bandwidth of the device compared to a bare NiTi wire in air. A Linear Parameter Varying (LPV) model provides 'snap-shot' views of the system characteristics. The primary discoveries of this model are demonstrated. Finally, benefits and downfalls of the Bowden tube system are discussed – both the qualitative and quantitative results show that this mechanical scheme provides significant benefits in applications where a strong actuator is needed with a small footprint, and when energy efficiency is not a concern.

BOWDEN TUBE SERVO DESIGN

A Bowden tube is a method for creating an antagonist force in a flexible package to transmit a reaction from one location to another (Figure 1). This is most commonly seen in bicycle push-pull cables: an external sheath is flexible but stiff in direct compression. Inside the sheath, a cable in tension is allowed to slide freely. Force is transferred from one end to the other by pulling on the cable while pushing on the sheath. Because the tensile and compressive loads are collinear along this entire Bowden tube, the tube can be bent or flex in any desired manner without interfering with the load transmission.
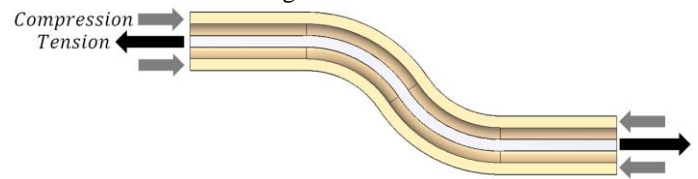
Figure 1. A typical 'Bowden Tube' mechanism transmits an equal and opposite reaction forces regardless of the tube's path or ending direction

In the SMA device, this same concept is used with small modifications (Figure 2). The inner cable is replaced with an SMA wire that strains when heated and cooled. One end of the wire is fixed to the tube; the other is free to slide in and out of the tube. This Bowden tube can be left slack, with all the motion near the active end. The slack can be coiled or pulled aside without affecting the strain of the SMA wire. By using PTFE (Teflon) tubing, a low-friction surface is provided to guide the SMA. When the SMA wire is small compared to the tube, any compression strain of the PTFE tube is negligible.
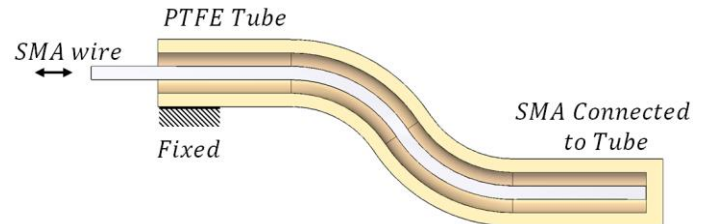
Figure 2. When used with SMA wire, the Bowden tube is held at the active end where the SMA wire will extend and contract. A long length of wire can be guided by the tube. The SMA wire and tube are connected at the other end.

The complete mechanism using this concept is shown in Figures 3 and 4. The main frame of the device is mounted in a fixed location where the actuator is desired. The Bowden tube is 200mm long, with 1/16" outer and 1/32" inner diameter (Figure 4). In operation, it is typically pulled to a convenient location or coiled up on itself. The 0.25mm NiTi wire runs the entire length of the tube, and is crimped into the electrical ground at the far end. At the active end, the NiTi wire is connected to a rocker which will rotate as the SMA contracts and extends (Figure 3). By connecting the electrical power source to the wire in air gap between frame and rocker, the rocker can be made from a common plastic such as ABS without risk of softening or melting. The antagonist force for the SMA wire comes from an elastic band on the opposite arm of the rocker. This antagonist arm is designed to provide a negative spring rate, slightly improving the working strain of the NiTi (see [21]). A socket-cap-screw (not show in the schematic) passes though the frame and rocker, and is bonded to the rocker with thin glue. This screw passes all the way through the frame and is tapered on the back end. Provisions

are made to connect a potentiometer on the back of the frame which rotates with the screw and rocker and provides angular position to the control computer. This particular potentiometer was taken from an electromagnetic RC servo and provides nearly 360 degree travel with very low frictional losses (Figure 6). Finally, the head of the screw is scored to match the splines of a common RC servo 'horn', which is the common method for connecting servos to loads which they push, pull or rotate (Figure 7).
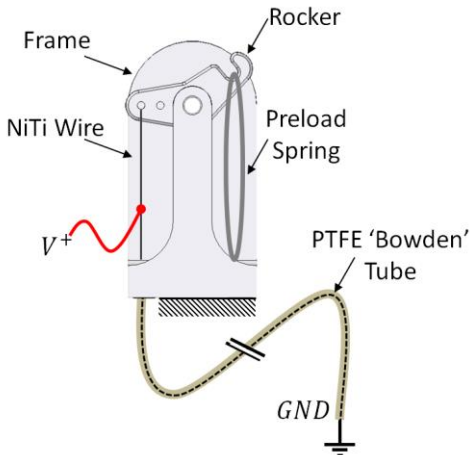
Figure 3. Schematic of the complete Bowden tube servo mechanism.
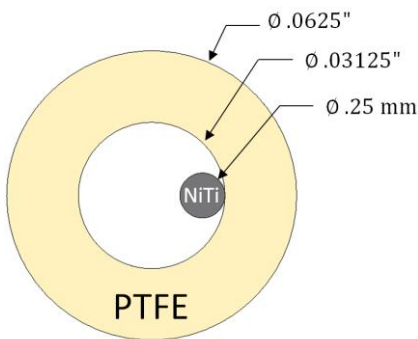
Figure 4. Dimensions of the PTFE tube and SMA wire inside it. Diameters are provided in inches. Total length is 200 mm.
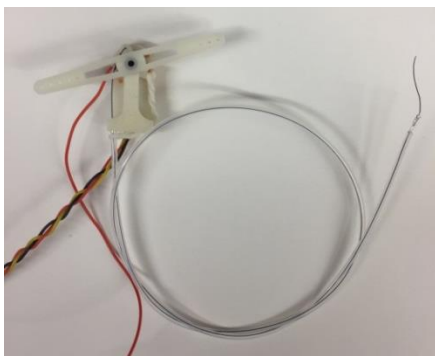
Figure 5. The prototype servo. The length of PTFE tube can be left slack or pulled out of the way to any convenient location. All activity happens at the small rotary servo end.
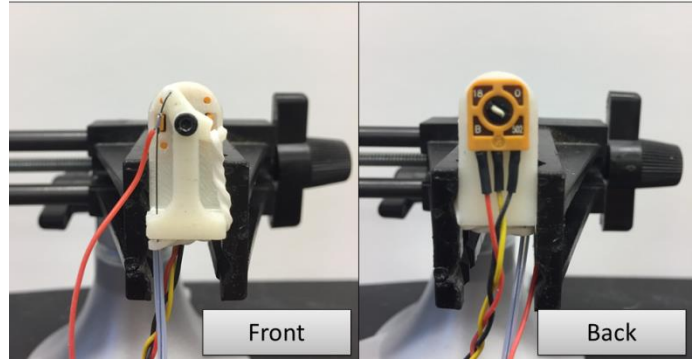
Figure 6. FRONT: Elastic band antagonist and SMA connection are shown. BACK: view of the feedback potentiometer.
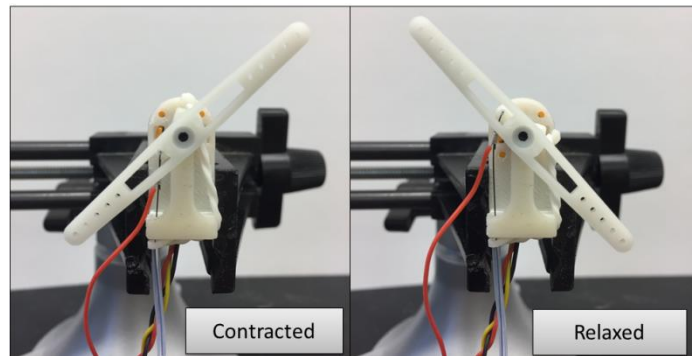
Figure 7. The full range of travel for the device is 90 degrees. A standard servo horn fits the formed screw head.

The 0.25mm SMA wire has an active length of 200 mm, providing a reliable linear stroke of 8mm, corresponding to a 90 degree swing of the rocker. This motion is centered such that the nominal range of motion is +/- 45 degrees – a common useful range of RC servos. Because the SMA acts directly on the rocker, the output torque (without any antagonist) is 49 N*mm (assuming an actuation stress of 180 MPa). The entire prototype Bowden tube servo mechanism weighs approximately 9.2 grams without wiring.

The electrical heating circuit contains a supervisor microcontroller and a simple MOSFET circuit to drive current through the SMA wire (Figure 8). The SMA wire is connected directly to a 5V power supply which can provide high current (as high as 2 Amp) and to the drain of a MOSFET. This MOSFET is an n-channel enhancement mode FET (FQP30N06L) which acts essentially like a solid-state switch; when voltage is applied to the gate it is closed and current flows through the NiTi wire. Otherwise, the FET 'switch' is open and no current flows. The voltage signal to activate the FET is provided by a microcontroller Pulse-Width-Modulated (PWM) signal. PWM signals can be generated by most common microcontrollers – the PWM signal approximates an adjustable voltage supply by varying the ratio of time spent turned ON to time spent turned OFF – the 'duty-cycle'. This PWM signal switches very quickly (several kHz), and so the SMA wire, with a bandwidth below ten Hz, reacts in a way similar to if the electric current is smoothly varied [22].
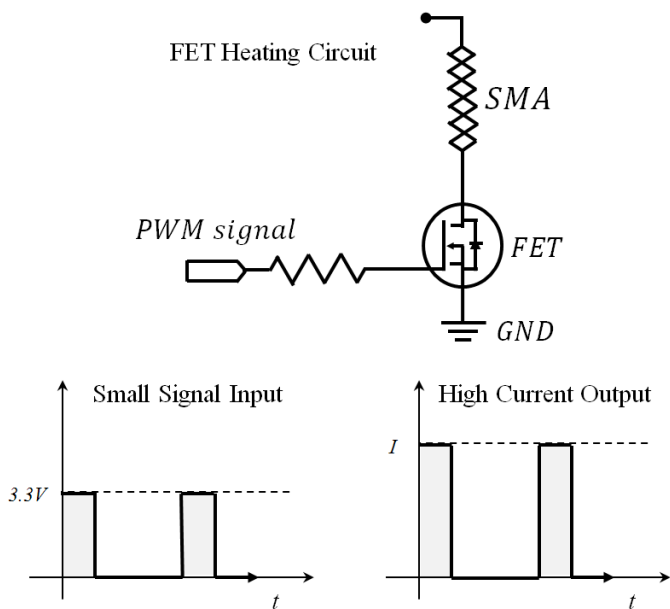
Figure 8. The circuit used to heat the SMA wire uses an n-channel MOSFET as a solid-state switch to control high current through the SMA wire

BANDWIDTH CHARACTERIZATION

Despite the clear mechanical benefits the Bowden tube will provide in some situations, it is not immediately clear how the tube will affect the actuation speed or bandwidth of the device. As with most NiTi devices, heat transfer speed is the limiting factor in bandwidth determination. A bare NiTi wire in air stores thermal energy internally via specific heat and latent heat of transformation (though the latter is sometimes ignored). It rejects heat to the environment solely through convection to the surrounding air. Adding a PTFE tube to the system has two complimentary effects: the total thermal capacitance is increased, but the convection rate rises due to larger surface area and fair conductivity through the material. With the physical prototype available, the most reliable method to determine the bandwidth change due to the Bowden system is direct comparison of the open-loop bandwidth, when tracking a sine sweep, with and without the tube sheath. The prototype device was modified to allow this experiment: for the 'bare' results, the wire was extended out from the servo frame and fastened 200 mm away, the entire wire was suspended in the air. Results for the complete Bowden tube servo system were measured with the tube allowed to hang loose from the servo frame, as would be common in practical applications. Figure 9 demonstrates the clear advantage of the tube in increasing bandwidth: while the Bowden tube can track (70%) at 0.1Hz, the wire in open air can only track at 0.08 Hz.
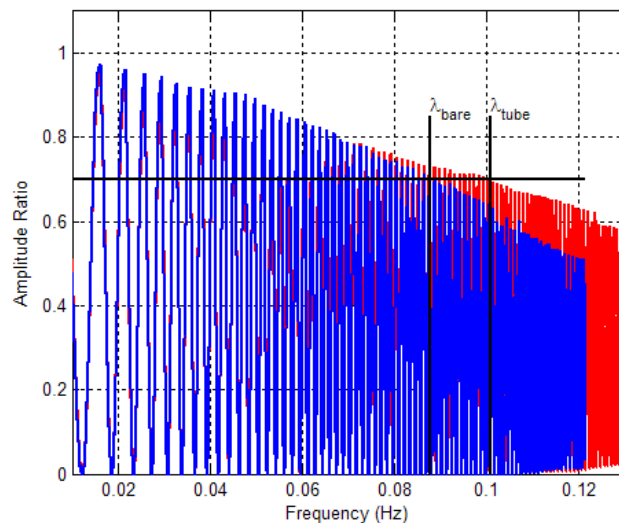
Figure 9. Comparison of performance between a bare wire in open air (0.08 Hz) and the Bowden tube (0.1 Hz). The tube increases the device speed.

However, this increase in bandwidth comes at a cost. Due to the increase in total mass being heated and cooled, the tube system requires more energy to operate. In Figure 10 the cycle time in open-loop is shown – this time with a step input rather than sinusoidal. When power is insufficient to heat both the tube and NiTi in a timely manner, the overall cycle time suffers. For the prototype device, the supply voltage had to exceed 9 Volts before the speed exceeded that of the wire in bare air. Beyond this critical point, the Bowden tube maintains approximately the same 20% advantage as seen in the bandwidth experiment.
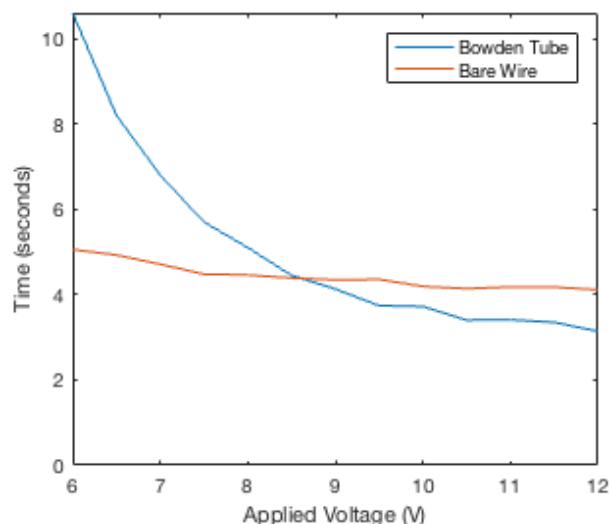
Figure 10. Increased bandwidth with the Bowden tube comes at a cost of high energy consumption. When little power is available, increased thermal mass (of the PTFE tube) leads to slow cycle time.

LPV MODELING AND SMC CONTROL

Linear Parameter Varying (LPV) models allow designers to apply well-known linear controls tools to nonlinear control problems such as SMA actuators. The nonlinear equations are written into a state space form, but instead of linearizing around an equilibrium point, the state matrices contain coefficients that change when some parameter of the system changes. In SMA actuators, the nonlinearity is entirely contained in the change of Martensite phase fraction – so the model varies based on the current phase fraction and its partial derivative with respect to temperature. In practice, the phase fraction cannot be measured during feedback control. The LPV model is used to design a sliding mode controller for the LPV device, ensuring it is stable in all situations. The most valuable discoveries of the LPV model are that heat transfer bandwidth is the dominant eigenvalue of the system, and varies widely due to the large effect of latent heat. Secondly, it is critical that a sliding mode controller use a second-order sliding surface design, because the SMA system has relevant 3rd order dynamics.

Underlying Model

To create a model that can be presented in LPV and used for control design, several simplifying assumptions are made about the material behavior
- The material properties and internal reaction forces are constant along the entire length of the wire
- Elastic modulus of the wire is constant
- Phase fraction is a function of temperature only

The model has three parts: SMA crystal phase behavior, controlled plant (system), and thermal behavior which contribute to the complete LPV system. The crystal phase fraction model has decades of pedigree. Some aspects of SMA phenomenological modelling are not debated, most researchers settle on constitutive models of the form:

$$\dot{\sigma} = E\dot{\epsilon} - E\epsilon_L\dot{\xi} - \Theta\dot{T} \qquad (1)$$

Where ϵ is strain, σ is stress, ξ is Martensite phase fraction, and T is temperature. The coefficients in this model are E, the elastic modulus, $\epsilon_L \approx 0.04$ the maximum shape memory strain with no load, and Θ the coefficient of thermal expansion. For actuators, the thermal expansion is small compared to the other terms and will be neglected hence. The constitutive relationships are clear – but they hide significant complexity in modelling the crystal phase fraction. In fact, one of the most explored topics in SMA modelling is selection of the kinetics model which relates temperature (and stress) to crystal phase fraction. The authors prefer a logistic function of the form:

$$\xi = \frac{\xi_m}{1 + \exp\big(k(T - C_m)\big)} \qquad (2)$$

Where C_m is the center temperature of peak transformation rate when transforming to Martensite (e.g. from DSC experiments), k is a fitting parameter that determines the width of the transformation temperature range, and ξ_m is a parameter which tracks the extent of transformation and provides a model of hysteresis in the material. The total model is framed in two parts to simulate the hysteresis

$$if \begin{Bmatrix} \dot{T} > 0 \\ \dot{T} < 0 \end{Bmatrix}$$

$$then \begin{cases} \xi_{M\to A} = \dfrac{\xi_M}{1 + \exp\big(K(T - C_A)\big)} \\ \xi_{A\to M} = 1 - \dfrac{\xi_A}{1 + \exp\big(-k(T - C_M)\big)} \end{cases}$$

$$and \begin{cases} \xi_A = (1 - \xi)\big(1 + \exp\big(-k(T - C_M)\big)\big) \\ \xi_M = \xi\big(1 + \exp\big(k(T - C_A)\big)\big) \end{cases} \qquad (3)$$

The mechanical system model combines the elastic portion of the SMA wire, as well as the mass (M), spring rate (K), and damping (B) in the mechanical system (Figure 11)

$$M\ddot{x} + B\dot{x} + Kx = -A\sigma = -AE(\epsilon - \epsilon_L\xi) \qquad (4)$$

This perspective of SMA control behavior is equivalent to considering the crystal phase strain ($\epsilon_L\xi$) as a physical movement pulling on an elastic member (the SMA wire) attached to the rest of the physical plant. In the Bowden servo system, the plant is primarily a damped mass, with a light preloading spring. In the physical actuator it is not necessarily the stress and strain we wish to control, but the total displacement (x) and the force (F). The material model is scaled by SMA cross-sectional area (A) and length (l) to accomplish this:

$$M\ddot{x} + B\dot{x} + Kx = F = -K_{sma}x + EA\epsilon_L\xi \qquad (5)$$

The effective spring rate of the SMA wire is $K_{sma} = AE/l$. Finally, the thermal model is taken to be a first order 'lumped-mass' model of the SMA wire and PTFE tube

$$c_{eff}\dot{T} = (P + hA_sT_\infty) - hA_sT \qquad (6)$$

$$c_{eff} = \left(m_{PTFE}C_{p_{PTFE}} + m_{SMA}\left(c_{p_{SMA}} + \Delta H\frac{\partial \xi}{\partial T}\right)\right)$$

This first-order differential equation relates the input heating power P to SMA temperature T, where m_{PTFE} is the mass of the PTFE tube, m_{SMA} the mass of the SMA wire, c_p their respective specific heats, ΔH the latent heat of transformation in NiTi, A_s the external surface area of the PTFE tube, and h is the heat transfer coefficient which has been shown experimentally to be near $121\,\text{W/m}^2\text{K}$. Notice that the effective thermal capacity c_{eff} varies with the phase fraction gain $\partial \xi/\partial T$.

Figure 11. The simplified view of SMA actuators which is used to derive the LPV system matrices

Linear Parameter Varying Perspective

Choosing the logistic function for a kinetics model has a distinct benefit of providing a clean partial derivative of ξ with respect to T

$$\frac{\partial \xi}{\partial T} = \frac{k\xi_m \exp(kx)}{(1 + \exp(kx))^2} = k\left(\frac{\xi^2}{\xi_m} - \xi\right) \quad (7)$$

The term $\frac{\partial \xi}{\partial T}$ contains the entire nonlinearity of the system, and takes the role as the single 'scheduling variable'. This relationship will be employed in the control design, noting that the time derivative of ξ is simply

$$\dot{\xi} = \frac{\partial \xi}{\partial T}\frac{dT}{dt} = \frac{\partial \xi}{\partial T}\dot{T} \quad (8)$$

The LPV model can be constructed from these final pieces. Using the exact velocity linearization method [23, 24], a third order state space model is constructed:

$$\begin{Bmatrix} \dddot{x} \\ \ddot{x} \\ \ddot{T} \end{Bmatrix} = \begin{bmatrix} 0 & 1 & 0 \\ -\dfrac{K_{sma} + K}{M} & -\dfrac{B}{M} & \dfrac{\frac{\partial \xi}{\partial T} EA\epsilon_L}{M} \\ 0 & 0 & -\dfrac{hA_s}{c_{eff}} \end{bmatrix} \begin{Bmatrix} \dot{x} \\ \ddot{x} \\ \dot{T} \end{Bmatrix} + \begin{bmatrix} 0 \\ 0 \\ \dfrac{1}{c_{eff}} \end{bmatrix} \dot{P} \quad (9)$$

This model has varying parameters in both the state-transition matrix and the input matrix. Because this single actuator is fairly simple, the authors find it convenient to consider the equivalent transfer function:

$$\frac{X}{P} = \left(\frac{1}{c_{eff}s + hA_s}\right)\left(\frac{\frac{\partial \xi}{\partial T}K_{sma}L\epsilon_L}{Ms^2 + Bs + (K + K_{sma})}\right) \quad (10)$$

The range of $\partial \xi/\partial T$ determines the variations that can be seen in the system model. When temperature is far from the transformation temperature, small changes in temperature have little effect on the phase fraction so $\partial \xi/\partial T$ is very small. The parameter has a maximum at $\xi = 1/2$. In all cases:

$$-.07 = -\frac{k}{4} < \frac{\partial \xi}{\partial T} < 0 \quad (11)$$

Where k was found experimentally for NiTi. The apparent eigenvalue of the heat transfer model (λ_1) varies greatly due to latent heat effects. Also, the gain on the applied power varies directly with change in $\partial \xi/\partial T$. Note that the eigenvalues from the mechanical system ($\lambda_{2,3}$) are not at all affected by the nonlinearity, though they would be if the elastic modulus was allowed to vary. The range of coefficients for the prototype system is shown in Table 1.

Table 1 - the range of coefficients in the LPV model, as $\partial \xi/\partial T$ is varied

	Minimum $\partial \xi/\partial T$	Maximum $\partial \xi/\partial T$
ξ	0 or 1	0.5
$\partial \xi/\partial T$	0	0.07
λ_1	-0.9273	-0.3064
$\lambda_{2,3}$	$-1.32 \pm 28i$	$-1.32 \pm 28i$

Another important revelation from the LPV model acts essentially like a third order system, where the slow heat-transfer pole dominates the speed of the system. Knowledge of the effective system order is critical to implementing a sliding mode controller that can stabilize the system.

Sliding Mode Control

When the characteristics of an SMA device are unknown, robust control techniques like Sliding Mode Control (SMC) are attractive solutions. Even when the parameters and characteristics of the SMA device are initially known, they might change through the life of the actuator, or in changing ambient conditions. The sliding mode controller is designed by creating a switching plane (in the phase space) with stable dynamics. A common method for selecting such a plane $\varsigma(x)$ is to use repeated negative real roots, which provides a stable plane for any desired system order:

$$\varsigma(x) = (s + \alpha)^{n-1} = s^2 + 2\alpha s + \alpha^2 \quad (12)$$

The sliding plane must be chosen to have order one degree lower than the controlled system order. For SMA the system is effectively third order, as seen in the previous section, so the design sliding surface must be second order. The sliding control law is easily implemented in an SMA system by switching the power on and off according to the equation:

$$u = -U * sign(s^2 + 2\alpha s + \alpha^2) \quad (13)$$

Where α is the defining root of the sliding surface which can be used as a tuning parameter, and U is the maximum voltage to be applied. For the Bowden tube servo system, $\alpha = 0.1$ was found to be effective – any choice near the heat transfer

bandwidth (Table 1) was stable, faster α choices prevent the controller from settling. The results of implementing this controller are shown in Figure 12. This controller provides very fast tracking in both directions (to the limit of the heating and cooling power available), and is generally robust to external disturbance.
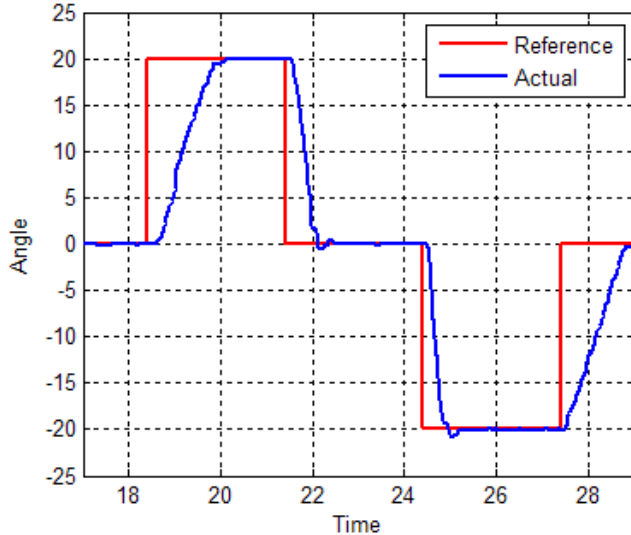
Figure 12. Tracking performance of the second order Sliding Mode Controller shows good performance with little overshoot

DISCUSSION AND CONCLUSION

The Bowden tube servo was found to provide significant benefits in providing a strong actuator with a small footprint. It allows a long length of wire to be incorporated without pulleys or parallel lengths of wire. Though not perhaps intuitive, the Bowden tube system cools faster than a bare wire in air, providing faster position control. The PTFE acts as a heat-sink to produce this effect, and so the improvement in speed cannot be separated from a simultaneous increase in power consumption and system mass. The sliding mode control system works well for the prototype system, providing reliable control even in the face of ambient air and torque disturbances. The LPV mode was able to guide critical design choice of 2nd order sliding surface and sliding mode bandwidth.

Future work for the mechanical system will involve refinement of critical dimensions. In particular, the PTFE tube will be analyzed to determine whether making it thinner (to reduce weight) will cause problems with deflection, or even slow the actuation speeds due to decreased surface area. The electronics will be packaged in a small, self-contained system similar to an RC servo, so that it can be more easily adopted by robot designers and other engineers.

Future work for the simulation and control will further leverage the model to design a gain-scheduled controller. The primary obstacle to this effort will be to determine the varying parameters in real life outside of simulation – perhaps using a state estimator or new measurement techniques. While not shown here, the choice of sliding surface order has a significant effect on stability if the appropriate 2nd order surface is not used. The effect will be demonstrated and shown in future work.

ACKNOWLEDGMENTS

REFERENCES

[1] L. Brinson and M. Huang, "Simplifications and Comparisons of Shape Memory Alloy Constitutive Models," *Journal of Intelligent Material Systems and Structures,* vol. 7, pp. 108-114, 1996.

[2] I. Chopra, "Review of State of Art of Smart Structures and Integrated Systems," *AIAA Journal,* vol. 40, no. 11, pp. 2145-2187, 2002.

[3] J. Jami, M. Leary, A. Subic and M. Gibson, "A review of shape memory alloy research, applications, and opportunities," *Materials and Design,* vol. 56, pp. 1078-1113, 2014.

[4] A. Paivo and M. Savi, "An Overview of Constitutive Models for Shape Memory Alloys," *Mathematical Problems in Engineering,* vol. 2006, no. 56876, pp. 1-20, 2006.

[5] S. Seelecke and I. Muller, "Shape memory alloy actuators in smart structures: Modeling and simulation," *ASME Applied Mechanics Review,* vol. 57, no. 1, pp. 23-46, 2004.

[6] C. Wright and O. Bilgen, "Analysis and Design of a Shape Memory Alloy Actuated Arm to replicate Human Biomechanics," in *Proc. ASME 2016 Conf. on Smart Materials, Adaptive Structures, and Intelligent Systems*, Stowe, 2016.

[7] P. Motzki, R. Britz and S. Seelecke, "Modular SMA-based Bi-directional Rotational Actuator," in *Proc. ASME 2016 Conf. on Smart Materials, Adaptive Structures, and Intelligent Systems*, Stowe, 2016.

[8] W. Coral, C. Rossi, J. Colorado, D. Lemus and A. Barrientos, "SMA-Based Muscle-Like Actuation in Biologically Inspired Robots: A State of the Art Review," in *Smart Actuation and Sensing Systems - Recent Advances and Future Challenges*, InTech, 2012, pp. 53-82.

[9] S. Shabalovskaya, J. Anderegg and J. Van Humbeeck, "Critical overview of Nitinol surfaces and their modifications for medical applications," *Acta Biomaterialia,* vol. 4, pp. 447-467, 2008.

[10] A. Nespoli and et al, "The high potential of shape memory alloys in developing miniature mechanical devices: A review on shape memory alloy mini-actuators," *Sensors and Actuators A: Physical,* vol. 158, pp. 149-160, 2010.

[11] A. Villoslada and et al, "High-displacement fast-cooling flexible Shape Memory Alloy actuator: application to an anthropomorphic robotic hand," in *14th IEEE_RAS int. Conf. on Humanoid Robots*, Madrid, 2014.

[12] A. Schiele, P. Letier, R. van der Linde and F. van der Helm, "Bowden Cable Actuator for Force-Feedback Exoskeletons," in *Proc. 2006 IEEE/RSJ Int. Conf. on Intelligent Robots and Systems*, Beijing, 2006.

[13] M. Elahinia, E. Esfahani and S. Wang, "Control of SMA Systems: Review of the State of the Art," in *Shape Memory Alloys: Manufacture, Properties and Applications*, Nova, 2010, pp. 49-68.

[14] M. Sreekumar, M. Singaperumal, T. Nagarajan, M. Zoppi and R. Molfino, "Recent advances in nonlinear control technologies for shape memory alloy actuators," *Journal of Zhejiang University SCIENCE A,* vol. 8, no. 5, pp. 818-829, 2007.

[15] A. Kilicarslan, K. Grigoriadis and G. Song, "Compensation of hysteresis in a shape memory alloy wire system using linear parameter-varying gain scheduling control," *IET Control Theory and Applications,* vol. 8, no. 17, pp. 1875-1885, 2014.

[16] C. Mehendale and K. Grigoriadis, "Hysteresis Compensation Using LPV Gain-scheduling," in *Proc. 2004 American Control Conference*, Boston, 2004.

[17] J. Jayender, R. Patel, S. Nikumb and M. Ostojic, "Modeling and Control of Shape Memory Alloy Actuators," *IEEE Transactions on Control Systems Technology,* vol. 16, no. 2, pp. 279-287, 2008.

[18] H. Ashrafiuon and V. R. Jala, "Sliding Mode Control of Mechanical Systems Actuated by Shape Memory Alloy," *J. Dynamic Systems, Measurement, and Control,* vol. 131, pp. 1-6, 2009.

[19] D. Grant, "Accurate and rapid control of shape memory alloy actuators," Centre for Intelligent Machines, McGill University, Montreal, 1999.

[20] D. Grant and V. Hayward, "Variable Structure Control of Shape Memory Alloy Actuators," in *IEEE International Conference on Robotics and Automation*, Nagoya, 1995.

[21] J. Swensen and A. Dollar, "Optimization of Parallel Spring Antagonists for Nitinol Shape Memory Alloy Actuators," in *IEEE Int. Conf. on Robotics and Automation (ICRA)*, Hong Kong, 2014.

[22] N. Ma and G. Song, "Control of shape memory alloy actuator using pulse width modulation," *Smart Materials and Structures,* vol. 12, pp. 712-719, 2003.

[23] M. Halas, M. Huba and K. Zakova, "The Exact Velocity Linearization Method," in *Proc. from the 2nd IFAC Conference*, Bratislava, 2003.

[24] D. Leith, "Input-output linearization by velocity-based gain-scheduling," *Int. J. of Control,* vol. 72, pp. 229-246, 1999.